International Journal of Radiation Biology, January 2015; 91(1): 81–89

ISSN 0955-3002 print / ISSN 1362-3095 online
DOI: 10.3109/09553002.2014.942013

informa
healthcare

Assessment of biological effectiveness of boron neutron capture therapy in primary and metastatic melanoma cell lines

Andrés E. Rossini[1,2], Maria A. Dagrosa[2,3], Agustina Portu[2,3], Giselle Saint Martin[2], Silvia Thorp[5,6], Mariana Casal[2,4], Aimé Navarro[1], Guillermo J. Juvenal[2,3] & Mario A. Pisarev[2,3,7]

[1]*Nuclear Regulatory Authority (ARN), Argentina,* [2]*Radiobiology Department, National Atomic Energy Commission (CNEA), Argentina,* [3]*National Council of Scientific and Technical Investigations, Argentina,* [4]*Oncology Institute "Ángel H. Roffo", University of Buenos Aires,* [5]*RA-3 Nuclear Reactor, CNEA, Buenos Aires,* [6]*Instrumentation and Control Department, CNEA, Buenos Aires, and* [7]*Department of Human Biochemistry, School of Medicine, University of Buenos Aires, Argentina*

Abstract

Purpose: **In order to optimize the effectiveness of Boron Neutron Capture Therapy (BNCT), Relative Biological Effectiveness (RBE) and Compound Biological Effectiveness (CBE) were determined in two human melanoma cell lines, M8 and Mel-J cells, using the amino acid p-boronophenylalanine (BPA) as boron carrier.**

Materials and methods: **The effects of BNCT on the primary amelanotic cell line M8 and on the metastatic pigmented melanoma cell line Mel-J were studied using colony formation assay. The RBE values were determined using both a gamma ray source, and the neutron beam from the Nuclear Reactor of the National Atomic Energy Commission (RA-3). For the determination of the RBE, cells were irradiated with increasing doses of both sources, between 1 and 8 Gy; and for the determination of CBE factors, the cells were pre-incubated with BPA before irradiation. Afterwards, the cell surviving fraction (SF) was determined for each treatment.**

Results: **Marked differences were observed between both cell lines. Mel-J cells were more radioresistant than the M8 cell line. The clonogenic assays showed that for a SF of 1%, the RBE values were 1.3 for M8 cells and 1.5 for Mel-J cells. Similarly, the CBE values for a 1% SF were 2.1 for M8 and 3 for Mel-J cell lines. For the endpoint of 0.1% of SF the RBE values obtained were 1.2 for M8 and 1.4 for Mel-J cells. Finally, CBE values calculated for a 0.1% were 2 and 2.6 for M8 and Mel-J cell lines respectively. In order to estimate the uptake of the non-radioactive isotope Boron 10 (^{10}B), a neutron induced autoradiographic technique was performed showing discrepancies in ^{10}B uptake between both cell lines.**

Conclusions: **These obtained in vitro results are the first effectiveness factors determined for human melanoma at the RA-3 nuclear reactor and show that BNCT dosimetry planning for patients could be successfully performed using these new factors.**

Keywords: Boron Neutron Capture Therapy (BNCT), Relative Biological Effectiveness (RBE), Compound Biological Effectiveness (CBE), borophenylalanine, melanoma

Introduction

Skin cancer is the third most common human malignancy, with more than 2 million estimated new cases around the world each year. Although melanoma only accounts for less than 5% of all cases, it is the most dangerous form and causes the vast majority of skin cancer deceases (Gray-Schopfer et al. 2007, Rigel 2010). In Argentina alone, more than 400 people die of melanoma each year (Loria et al. 2008).

If detected early, melanoma can be treated with surgical resection. However, in its most advanced stages, its frequent resistance to conventional radiotherapy and chemotherapy has led to active research for more effective modalities and to the application of alternative solutions (Dean and Lorigan 2012, Mackiewicz-Wysocka et al. 2013). Since phase I/II melanoma Boron Neutron Capture Therapy (BNCT) clinical trial was approved in Argentina in 2003, seven patients presenting multiple subcutaneous skin metastases of melanoma in their extremities have been treated (Menéndez et al. 2009).

BNCT is a binary radiation treatment modality with the potential to selectively target cancer cells. A non-toxic compound containing atoms of the stable isotope of boron (^{10}B) is selectively and actively incorporated into tumor cells. These ^{10}B atoms irradiated with thermal neutrons produce ^{11}B in an unstable form, which then undergo instantaneous nuclear fission to produce high-energy α particles and recoiling lithium (^{7}Li) nuclei (Coderre and Morris 1999, Barth et al. 2012). These heavy charged particles have very short path lengths comparable to cancer cell dimensions, and deposit most of their energy within the ^{10}B-containing cells. As a result, individual cancer cells are selectively killed without serious injury to the surrounding normal tissue (Coderre and Morris 1999, Coderre et al. 2003).

Unlike conventional radiotherapy modalities, the radiation field during BNCT consists of a mixture of components

Correspondence: Dr Andrés E. Rossini, MSc, Laboratory of Radiation Pathology, Nuclear Regulatory Authority (ARN), Presbítero Juan González y Aragón 15, (B1802 AYA) Ezeiza, Buenos Aires, Argentina. Tel: + 54 11 6779 8263. Fax: + 54 11 4125 8373. E-mail: rossini@arn.gob.ar

(Received 28 January 2014; revised 22 June 2014; accepted 27 June 2014)

with different Linear Energy Transfer (LET) characteristics. Therefore, the total absorbed dose will be the sum of the physical doses from the different types of radiation. To express the total BNCT dose in terms that allow a comparison with conventional photon treatments, each radiation component must be multiplied by an appropriate Relative Biological Effectiveness factor (RBE) (Coderre et al. 1993, Wambersie and Menzel 1993). In the case of the BNCT, it is necessary to take into consideration the 'classical' RBE for the neutron source and an effectiveness factor for the ^{10}B capture reaction products, that result from the ^{10}B (n,α) ^{7}Li reaction, termed Compound Biological Effectiveness (CBE) (Coderre and Morris 1999, Barth et al. 2005).

The currently available software (NCTPlan treatment planning system and the DVH Tool system) (González et al. 2004) for the treatment planning and clinical implementation of BNCT, enables the calculation of the total biologically equivalent BNCT absorbed doses (Gy-Eq) in normal skin and in the tumor. However, until now, there is no available data on RBE or CBE for BNCT of the neutron source in our reactor using the amino acid p-boronophenylalanine (BPA) as boron carrier. Therefore, and as a preliminary assessment in vitro, the RBE of the RA-3 neutron source and the CBE for the boron carrier BPA were determined using two selected cell lines with completely opposite characteristics, especially regarding their radiosensitivity and melanin content: M8, which is an amelanotic primary human melanoma cell line, and Mel-J, which is derived from metastatic pigmented melanoma cells.

The responses obtained in the study from a clinical theoretical simulation; using these new RBE and CBE effectiveness factors as inputs, indicate a therapeutic ratio in support of BNCT compared to the therapeutic benefit obtained with a conventional photon-radiation modality.

In order to assess the performance of this new set of in vitro effectiveness factors, Gy-Eq photon doses were calculated within a theoretical clinical simulation using the currently available software for the treatment planning and the clinical implementation used during BNCT clinical trial of melanoma conducted in Argentina (González et al. 2004).

However, even when these new factors succeed in amplifying the skin tolerance dose for achieving far exceed the tumor dose control, a major problem in BPA-based BNCT is the lack of precise and detailed knowledge regarding realistic intracellular ^{10}B levels. Since energetic α/lithium particles through ^{10}B (n,α)^{7}Li reactions are responsible for most part of the lethal damage to tumor cells during BNCT, the information on boron compound concentration and distribution patterns within cells would be very significant in relation to the studies of the CBE factor and hence, to the efficacy of BNCT treatments. It is largely believed that one of the major limitations for BNCT effectiveness is the insufficient incorporation of ^{10}B into tumor cells (Coderre and Morris 1999). Therefore, a deeper understanding of the BPA uptake and efflux mechanisms into and from the tumor cells might allow a specific modification on those processes in order to obtain a higher concentration of ^{10}B in the tumor cells and a greater effectiveness of BNCT.

Several groups of investigators have suggested the group of the neutral amino acid transporters (system L) as the main responsible implicated in the BPA transport process across cell membranes (Papaspyrou et al. 1994, Imahori et al. 1998, Wittig et al. 2000). At present, four transporter subtypes that generate Na^{+}- independent amino acid transport (system L-type) have been cloned: LAT1-4F2hc, LAT2-4F2hc, LAT3 and LAT4. At the molecular level, the LAT1 and LAT2 transporters are heterodimers composed of a heavy-chain glycoprotein (4F2hc) and a catalytic light chain (LAT1/LAT2) that are covalently linked by a disulphide bond (Kanai et al. 1998, Pineda et al. 1999). These transporters function as obligatory exchangers with a 1:1 stoichiometry, and the activity of transport depends on the availability of a pool of intracellular substrate amino acids. This means that net transport of a given amino acid can be obtained only in exchange for other amino acids that might have been taken up by another (unidirectional) transport system. On the other hand, LAT3 and LAT4 do not require co-expression with 4F2hc. Unlike LAT1 and LAT2, these two proteins are monomeric subunits with intrinsic catalytic activity and exhibit narrow substrate selectivity (Babu et al. 2003, Bodoy et al. 2005).

The issue of the efficiency of the BPA uptake is particularly important, consequently, and in order to determine the uptake and distribution of ^{10}B within cells, a neutron-induced autoradiography with solid State Nuclear Track Detectors (SSNTD) technique was performed for both cell lines. The application of the autoradiographic technique showed considerable differences in the intracellular ^{10}B concentration between cell lines.

Materials and methods

Human cell lines

The M8, an amelanotic cell line derived from a primary cutaneous melanoma and Mel-J, a pigmented cell line established from a metastatic melanoma lesion of the lung (Guerra et al. 1989) were routinely grown in plastic culture flasks (80 cm^2; Greiner Bio-One, Monroe, NC, USA) using RPMI-1640 medium (Gibco, Grand Island, NY, USA) supplemented with 10% fetal bovine serum (Natocor, Carlos Paz, Córdoba, Argentina) and incubated at 37°C in 5% CO_2 atmosphere. Cell lines were kindly provided by Dr A. Baldi (Institute of Biology and Experimental Medicine IByME, Buenos Aires, Argentina). For irradiation experiments, cells were seeded in T-25 bottles (25 cm^2; Greiner Bio-One, Monroe, NC, USA) under routine growth conditions, and transported to the RA-3 reactor for neutron irradiation and to the Angel Roffo Oncology Institute for gamma irradiation.

Preparation of boron solutions

The boronated amino acid BPA was purchased from Boron Biologicals Inc. (BBI, Raleigh, NC, USA). The stock solution of BPA-fructose was prepared at a concentration of 30 mg BPA per ml (0.14M). The BPA (95% ^{10}B enriched, L-isomer) was combined in water with 10% molar excess of fructose (Sigma-Aldrich, St Louis, MO, USA) to increase its solubility.

The pH was adjusted to 9.5–10 with NaOH, and the mixture stirred until all solids were dissolved. The pH was readjusted to 7.4 with HCl.

Gamma irradiations and clonogenic assays

Exponentially growing cells, seeded 24 h before irradiation, were distributed into the following groups: (1) Gamma rays, (2) neutrons only, (3) neutrons + BPA ($^{10}B = 10$ ppm or 10 μg ^{10}B/ml medium) and controls: (4) BPA and no irradiation, (5) no BPA and no irradiation. After irradiation, each group of cells was assayed for clonogenic survival (Franken et al. 2006) and the cell surviving fraction (SF) was considered as the endpoint (0.1% and 1% of SF).

For the first group, gamma irradiation was performed using a ^{60}Co source from the Angel H. Roffo Institute of Oncology at a dose-rate of 1.25 Gy/min. For groups 2 and 3, the nuclear reactor RA-3 with 8 MW power was used as a thermal neutron source. This facility provides quite a uniform thermal neutron flux with negligible contribution from fast neutrons. A more detailed description of the thermal neutron field characterization and dosimetry procedures can be found in Miller et al. (2009).

The intrinsic radiation sensitivity was expressed by the surviving fraction at 2 Gy (SF_2). For the studies with ^{10}B, cells were incubated with a volume of BPA stock solution in order to obtain 10 μg/g ^{10}B (0.925 mM BPA) in medium culture. After 2 h incubation, cells were irradiated. Incubation times were selected taking into account previous studies performed on these cell lines (Carpano et al. 2010). Control groups were performed by incubating the cells with BPA for the same period of time but without irradiation. Irradiation times were calculated in order to deliver doses of 1, 3, 5 and 8 Gy with an uncertainty of 10%.

The number of cells to seed in each group and for each radiation dose was adjusted in order to obtain 50–200 colonies. Dishes were incubated at 37°C for 11 days for Mel-J cells and 12/13 days for M8 cell line in an atmosphere of 5% CO_2 and 95% air. At the end of this period of time, bottles were rinsed with Phosphate Buffered Saline (PBS) and stained with a solution of 5% crystal violet in methanol (25%). Colonies containing at least 50 cells were counted.

As there is no reliable method to measure the boron intracellular concentration in vitro at the time of irradiation, we assumed that BPA was uniformly distributed inside and outside the cells for the dosimetric calculations (Fukuda et al. 1994, Coderre and Morris 1999).

The dose-surviving fraction data was fitted using a linear-quadratic (L-Q) model using Origin 7.0 data analysis and graphics software (OriginLab Corporation, Northampton, MA, USA).

Neutron irradiation and determination of RBE and CBE values

Surviving fraction data were plotted against total absorbed dose (Gy). Dose-response curves were fitted to the cell survival data by the method of least squares using the L-Q model with Origin 7.0 data analysis and graphics software. The RBE of the beam and the CBE for BPA were determined for two different levels of surviving fraction, SF = 0.01 and SF = 0.001 (1% and 0.1% of cell survival, respectively).

The neutron beam RBE value was obtained by irradiating in the absence of boron and comparing the neutron beam dose with the γ-ray dose sufficient to produce a SF of 1% and 0.1% as described in Equation 1.

$$RBE = \frac{Dose\,\gamma}{Dose\,beam} \quad (1)$$

To express the total BNCT dose in a common photon equivalent unit, each of the BNCT dose components is multiplied by an effectiveness factor as described in Equation 2 (Coderre and Morris 1999).

$$Dose\,\gamma = Dose_{beam} \times RBE + {}^{10}B\,Dose \times CBE \quad (2)$$

Solving Equation 2 for the CBE factor produces Equation 3

$$CBE = \frac{Dose\,\gamma - (Dose\,beam \times RBE)}{{}^{10}BDose} \quad (3)$$

With the purpose of evaluating the performance of this new set of effectiveness factors, Gy-Eq photon doses were calculated within a theoretical clinical simulation using the NCTPlan treatment planning system and the DVH Tool system (González et al. 2004), the software currently available for the treatment planning and the clinical implementation used during BNCT clinical trial of melanoma conducted in Argentina (Menéndez et al. 2009). The theoretical simulation was performed using RBE and CBE factors determined in vitro for both cell lines corresponding to a SF of 0.1%.

During the theoretical dosimetry planning, the maximum tolerated dose for normal skin (MTD_{skin}) was set at 24 Gy-eq according to the tolerance dose estimated as the upper limit for BNCT procedures (Fukuda et al. 1994, González et al. 2004). According to the BNCT protocol-based procedure for the treatment of cutaneous melanomas designed by the National Atomic Energy Commission of Argentina and the Ángel H. Roffo Oncology Institute, the relative contribution of ^{10}B dose component in relation to the total absorbed dose in normal skin is taken into account as well as the contaminant gamma component (see Table I) and all the other sub-components originated from thermal neutrons capture reactions. The combination of all these components will represent the MTD_{skin}. Thus, based on the results reported by Fukuda et al. (1994), a MTD_{skin} of approximately

Table I. Radiation survival curves parameters and the plate efficiency (PE).

Cell line	Treatment	SF_2 (Gy)	D_{37} (Gy)	α (Gy^{-1})	β (Gy^{-2})	PE (%)
M8	γ	0.3	1.6	0.46 ± 0.04	0.096 ± 0.008	62
M8	n	0.1	0.9	0.96 ± 0.05	0.05 ± 0.01	42
M8	n + BPA	0.04	0.8	1.10 ± 0.10	0.17 ± 0.05	34
Mel-J	γ	0.8	4.6	0.06 ± 0.05	0.032 ± 0.008	57
Mel-J	n	0.5	2.4	0.33 ± 0.07	0.04 ± 0.01	32
Mel-J	n + BPA	0.2	1.3	0.62 ± 0.03	0.08 ± 0.02	37

SF2, surviving fraction at 2 Gy; D37, The dose at which 37% of the cells survive; PE, Plate efficiency.

18 RBE-Gy and minimum dose for tumor control of 24 RBE-Gy are assumed (Blaumann et al. 2004).

Neutron autoradiography

In essence, the autoradiographic technique employed in this work was in accordance with the method developed by Amemiya et al. (2005) and Konishi et al. (2007). Such method enables the simultaneous visualization of mammalian cells as a relief on a plastic track detector, CR-39 (Armorlite, San Marcos, CA, USA) and the etch pits which indicate the positions of alpha particles produced by (n, alpha) reaction after neutron irradiation.

Cells were seeded on CR-39 foils placed at the bottom of p60 plates (Greiner Bio-One, Monroe, NC, USA), under the same conditions as those for routine growth. Growing cells at 50/60% of confluence were exposed to thermal neutrons at a fluency of 10^{13} n cm^{-2}. The irradiated samples were exposed to 254 nm ultraviolet radiation (UV) for 4 h. Afterwards, they were haematoxylin stained and photographed with a charged coupled device (CCD) camera (Olympus DP70, Shinjuku, Tokyo, Japan), and etched in alkaline solution of 7N NaOH at 60°C for 20 seconds. Both etch pits of the nuclear tracks, coming from alpha particles and Li ions originated by the capture reaction and the relief of culture images produced by transmitted UV were observed on the detector foil surface with a conventional light microscope.

Statistical analysis

Statistical analysis was performed using Student's *t*-test for number of tracks per cell comparisons. Differences were considered significant at $p < 0.05$.

Results

Resistance to radiation

The cell survival curves are shown in Figures 1 and 2 for M8 and Mel-J, respectively. The cell survival curve parameters and the Plate Efficiency (PE) are presented in Table I together with the SF_2 and the radiation dose required for 37% survival (D_{37}). The results showed that cells were markedly different with regard to cellular radiosensitivity. Survival at 2 Gy for γ-rays was 80% for Mel-J and 30% for M8 cells. In the case of the neutron beam, it was 50% for Mel-J and 10% for M8 cells; and for neutrons in the presence of BPA, the survival was 20% and 4% for Mel-J and for M8 respectively (Table I, Figures 1 and 2).

The D_{37} values for metastatic Mel-J cells were 4.6 Gy for γ-rays, 2.4 Gy for neutron beam only and 1.3 Gy for neutrons plus BPA. In contrast, the D_{37} values for non-metastatic M8 cells were 1.6 Gy for γ-rays, 0.9 Gy for neutron beam only and 0.8 Gy for neutrons plus BPA. These parameters represent fundamental differences in radiosensitivity, indicating that metastatic Mel-J cells are clearly more resistant to radiation than M8 cells.

Effectiveness factors

Neutron irradiation, either in the presence or absence of boron, was more effective than ^{60}Co γ-rays irradiation. This effect was markedly greater in cells incubated with BPA (Figure 1 and Figure 2).

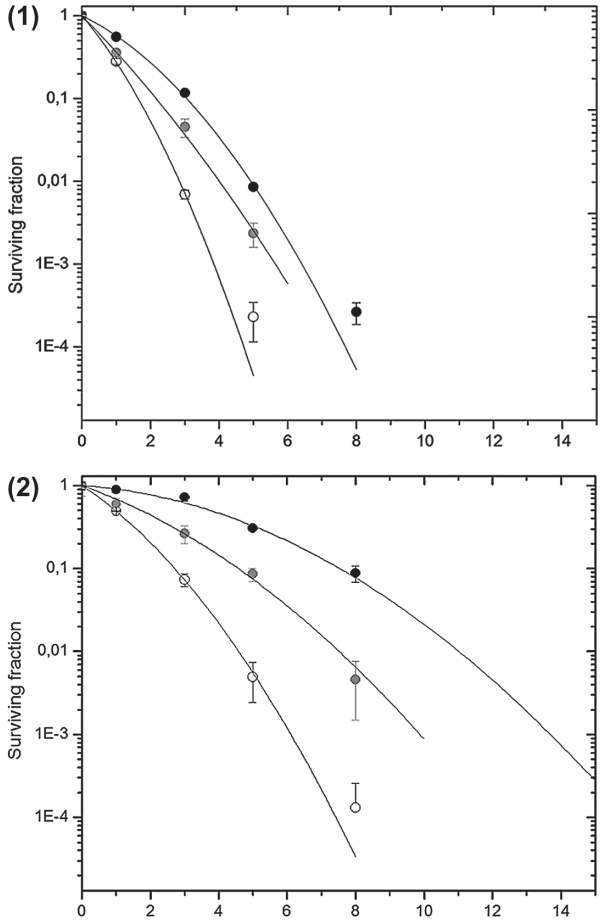

Figures 1 and 2. M8 and Mel-J survival curves: Dose-related changes in the surviving cell fraction of primary amelanotic M8 cell line and pigmented metastatic melanoma cell line Mel_J. (●) gamma rays, (●) neutron beam (including gamma-contaminant component) and (○) neutron beam in presence of 10 μg/g of ^{10}B. Each data point with vertical line represents the mean value and standard deviation. Each point is the average of 8 plates ± SD of two different experiments. Data are fitted to a linear quadratic model, $SF = e^{-(\alpha D + \beta D2)}$. As goodness of fit the R^2 was considered. For M8 R^2 of the survival curves obtained were: 0.990 for gamma rays, 0.996 for neutron beam only and 0.995 for neutron beam plus BPA. For Mel-J, the R^2 obtained were 0.983 for gamma rays, 0.974 for neutron beam only and 0.999 for neutron beam plus BPA (10 μg/g ^{10}B).

Table II shows the corresponding dose components (contaminant γ dose component of the neutron beam ($f\gamma$), ^{14}N neutron beam component (fn) and ^{10}B component ($f\,^{10}$B) of the total physical absorbed dose for each irradiation treatment in presence of BPA. These dose components can be expressed as partial contributions (f) of the total physical absorbed dose (f_{total}) being $f_{\text{total}} = f\gamma + f\text{n} + f\,^{10}\text{B}$. Assuming f_{total} as a unity, the proportional partial contributions of each component to the total physical absorbed dose would be 0.17, 0.2 and 0.63 for $f\gamma$, fn and $f\,^{10}$B respectively (see Table II).

For the neutron beam, RBE values of 1.2 and 1.3 were obtained from M8 cells and values of 1.4 and 1.5 from Mel-J for endpoints of 0.1% and 1% of SF respectively (Table III). It is worth noting that these RBE factors have been calculated for the neutron beam including the gamma-contaminant component; hence, the RBE values for pure neutrons are

Table II. Dosimetry of cells growing in presence of BPA in culture. Total physical absorbed doses (1, 3, 5 and 8 Gy) were delivered for both cell lines and used for the plot of survival curves.

Cell line	Boron (ppm)	γ component (Gy)	^{14}N component (Gy)	^{10}B component (Gy)	Total physical absorbed dose (Gy)
M8	10	1.34	1.62	5.04	8.00
	10	0.84	1.02	3.16	5.02
	10	0.5	0.61	1.88	2.99
	10	0.17	0.20	0.63	1.00
Mel-J	10	1.36	1.61	5.02	7.99
	10	0.85	1.00	3.14	4.99
	10	0.51	0.60	1.88	2.99
	10	0.17	0.20	0.62	1.00

BPA, p-boronophenylalanine; 10B, boron 10; ppm, parts per million; Boron concentration = 10 ppm10B = 10 μg 10B/ml; culture medium = 0.925 mM BPA in medium. Gamma (γ), 14N and 10B sub-doses represent the partial contribution (*f*) of each component to the total physical absorbed dose being 16%, 21% and 63% the contributions of γ component, 14N component and 10B component, respectively.

higher. For CBE factors the values obtained were 2 and 2.1 for M8 cells and 2.6 and 3 for Mel-J cell line for 0.1% and 1% of SF, respectively, as shown in Table III.

The partial contributions (*f*) of the dose components to the total BNCT doses at the RA-3 reactor for a thermal neutron flux of 7.5 10^9 n/cm^2 sec are detailed in Table IV. The RBE and the CBE factors included are those corresponding for 0.1% of cell survival and used for the calculations of the equivalent doses.

Theoretical simulation using the in vitro effectiveness factors

We found that when these new RBE and CBE values determined in vitro were used as the biological inputs required for simulating a theoretical dosimetry planning, the tolerance limit of the surrounding normal skin resulted in amplified photon equivalent doses in tumor cells that far exceed the minimum doses required for tumor control.

In the case of amelanotic M8 cells, the MTD became into a total physical absorbed dose of 36.7 Gy-eq and for the pigmented cell line Mel-J, the MTD would come to a total physical absorbed dose of 47.4 Gy-eq.

Neutron autoradiography

The method adapted from the technique published by Amemiya et al. (2005) is based on the fact that the etching speed of CR-39 is enhanced by UV exposure. After UV irradiation, relief images of the cell cultures' growth on the CR-39 surface and of etch pits by neutron-induced α-particles were simultaneously recorded on the track detector surface. The α/lithium-tracks autoradiography observed on the CR-39 surface reproduced the BNCT events, allowing the confirmation of ^{10}B presence within cells, as shown in Figures 3 and 4.

It was found that after counting 20 random fields for each cell line, the average tracks per cell were 15 tracks for Mel-J cells and 8 tracks for M8 cells ($p < 0.05$). Considering these results and the average cell areas for each cell line, the estimation of ^{10}B uptake were of 2.6 for Mel-J and 0.7 for M8 cells. These results are expressed as the relationship between the intracellular and extracellular track densities. The extracellular value of track density was obtained by counting the number of track per unit area of a 10 ppm ^{10}B solution in contact with the SSNTD.

Discussion

Cellular radiosensitivity

In the present study the radiobiological characteristics of two human melanoma cell lines, M8 originated from a primary cutaneous melanoma and Mel-J derived from a human lung metastasis, were analysed. It could be concluded that Mel-J cells were more resistant to both γ rays and neutrons than M8 cells, and that neutron beam was more efficient than γ rays in their killing potential.

Several reports in literature have shown that there is a great variation in the radiosensitivity between cell lines. Correlation between radioresponsiveness and growth rate, distribution of cells in the different phases of cell cycle, repair of potentially lethal damage and response to radiation was described in several studies (Selzer and Hebar 2012).

The distribution of cells in the different phases of the cycle is influenced by the rate of proliferation, and the radiosensitivity variation during the cell cycle affects the radioresponsiveness of cells. Mel-J is a highly heterogeneous cell line characterized by the presence of small round cells, multicellular aggregates, polydendritic cells and giant mega-cells resembling the different stages of melanocytic

Table III. RBE and CBE factors for M8 and Mel-J cell lines following thermal neutron irradiation in combination with BPA and thermal neutron beam alone.

Irradiation	Cell line	RBE $SF_{0.001}$	RBE $SF_{0.01}$	CBE factor $SF_{0.001}$	CBE factor $SF_{0.01}$
N beam only	M8	1.2	1.3	–	–
N beam + BPA	M8	–	–	2	2.1
N beam only	Mel-J	1.4	1.5	–	–
N beam + BPA	Mel-J	–	–	2.6	3

N beam, thermal neutrons beam; BPA, p-boronophenylalanine; SF, survival fraction.

Table IV. Effectiveness factors corresponding for 0.1% of cell survival and partial contributions (f) of each dose component to the total doses for BNCT treatments used for the theoretical simulation.

	Skin	M8	Mel-J
RBE beam	–	1.2	1.4
CBE	2.5*	2	2.6
RBE n	3*	1.38	1.75
f n	0.124*	0.063	0.063
$f\gamma$	0.109*	0.055	0.055
f^{10}B	0.788*	0.881	0.881

*Clinical values from literature (Fukuda et al. 1994, Menéndez et al. 2009). f contributions of each dose component to the total dose; f n dose fraction corresponding to neutrons only; f γ dose fraction corresponding to gamma rays; f 10B dose fraction corresponding to 10B; RBE beam Relative Biological Effectiveness calculated for the neutron beam including the gamma-contaminant component; RBE n, Relative Biological Effectiveness calculated for neutrons only.

differentiation (Guerra et al. 1989). Cytogenetic analysis of Mel-J revealed extensive chromosomal alterations, including a highly heterogeneous chromosome number and chromosomal rearrangements, gains, losses and isochromosomes. This highly heterogeneous cell line should be considered an excellent model to study cellular differentiation and interaction between different subpopulations in human melanoma. This heterogeneity of different genotype-phenotype subpopulations causes cell cycle desynchronization in this cell line, resulting in a doubling time of total cell population of 70–80 h (Guerra et al. 1989) which is relatively high for a cancer cell line and almost twice as long as the doubling time of M8 cells. Repair of potentially lethal damage is more important in cells with a large number of quiescent cells than in those where a large proportion of the cells are proliferating rapidly. Quiescent cells are more radioresistance than cells in cycle.

Another singular characteristic of Mel-J cells is their marked aneuploidy showing diploid, triploid and tetraploid cell subpopulations (Guerra et al. 1989). Furthermore,

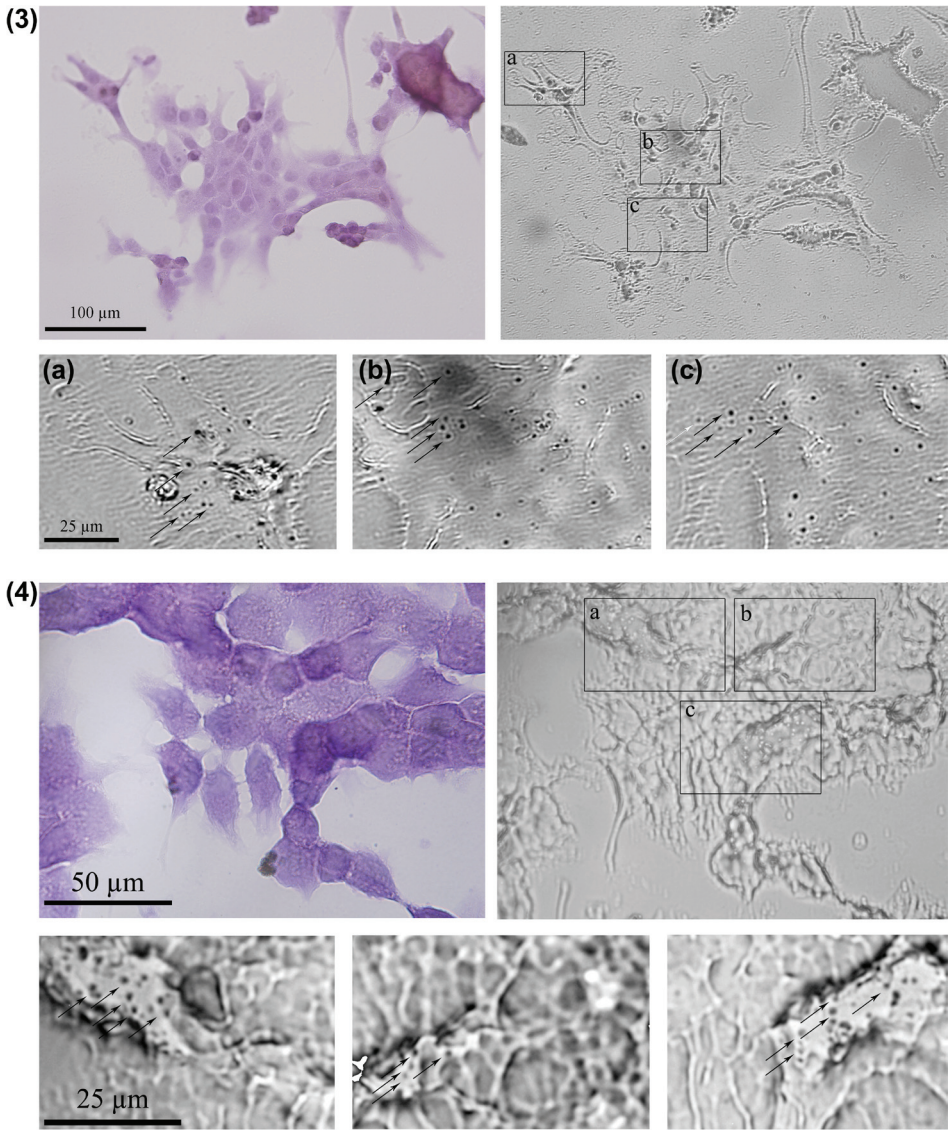

Figures 3 and 4. Neutron-induced α-autoradiographies in M8 and Mel-J melanoma cell lines after 2 hours of incubation with BPA. Figure 3 upper left panel: M8 cells cultured on polymeric nuclear track detector (SSNTD) before the etching process in alkaline solution (stained with hematoxylin). Figure 3 upper right panel: Same image after the etching process with alkaline solution. Selected areas (a, b and c) highlight portions of the cell culture with high density of tracks. Figure 4 upper left panel: Mel-J cells cultured on polymeric nuclear track detector (SSNTD) before the etching in alkaline solution (stained with hematoxylin). Figure 4 upper right panel: Same image after the etching process with alkaline solution. Black arrows indicate examples of etch pits in relief corresponding to the α/lithium particles generated from neutron capture reactions ^{10}B (n,α) ^{7}Li of ^{10}B within cells (not all tracks are indicated). This Figure is reproduced in color in the online version of *International Journal of Radiation Biology*.

the Mel-J cell line and most tumors are also characterized by the presence of subpopulations of cells of different metastatic potential. Several studies have shown that genetic alterations during progression of melanoma to increased levels of malignancy are implicated in the development of drug and radiation resistance, and therefore, cellular radiosensitivity may differ significantly between primary tumors and metastatic tumors (Rofstad 1992, van den Aardweg et al, 2002).

Biological effectiveness factors

Up to now, in the absence of more realistic biological effectiveness factors of BPA-based BNCT of melanoma and particularly for the RA-3 reactor, the RBE and CBE factors adopted in Argentina were those determined by Fukuda et al. (2003) for the Musashi Institute Technology Reactor (Kawasaki, Japan) and since 1996 for the Kyoto University Reactor (KUR, Kumatory Japan). However, the results of the theoretical dosimetry planning in this study showed that the effectiveness factors determined in vitro for the RA-3 reactor could be used during clinical practice. Moreover, the determined CBE factors demonstrated a marked therapeutic benefit either for a primary cell line such as the M8 cells, as well as for an aggressive metastatic cell line like Mel-J, even when the CBE factors were quite different for this two cell lines.

Regarding the BPA-based CBE values for cells in culture, given the short range of alpha particles and the ^{7}Li particles, variations of this parameter are directly related to the ^{10}B concentration and microdistribution within cells (Santa Cruz and Zamenhof 2004). Furthermore, the parameters related with cellular morphology and cellular metabolism such as the number of nuclei per cell; size, shape and average diameter of the nuclei; nuclear/cytoplasmic ratio; stage of cell cycle; melanin content and in particular the gene expression level of the transporters responsible for BPA uptake are among the parameters that may influence the experimental determination of the CBE factors (Coderre and Morris 1999, Suzuki et al. 2000). The CBE is thus a complex multifactorial parameter and expresses the efficiency of dose delivery to a defined anatomical target.

The success of BNCT depends on the preferential uptake of boron by the malignant cells (Barth et al. 2012). In the case of BPA selective uptake, it is thought to be enabled by the system L family of heterodimeric amino acid transporters, in particular by LAT1, located at the plasma membrane (Wittig et al. 2000). LAT1 has been associated with growth and proliferation, is highly expressed in malignant tumors and cancer cell lines, and it has been proposed as a novel independent biomarker of high-grade malignancy to assess prognosis in some types of cancer (Kaira et al. 2009, Yanagisawa et al. 2012). However, it should be mentioned that to date, no study of the role of the alternative subunits of system L transporters, also responsible for BPA uptake described in the literature (LAT2, LAT3 and LAT4) has been performed in the field of BNCT (Rossini et al. 2010).

In the BNCT field several studies pointed to a direct relationship between the uptake of BPA and cell replication. Ono et al. (1996) studied the distribution of boron compounds at the subcellular level using a squamous cell carcinoma mouse model and concluded that the distribution of BPA was heterogeneous and that quiescent cells may not accumulate BPA. Another study by Yoshida et al. (2002) was focused on the differences in BPA uptake by tumor cells in different phases of the cell cycle, showing higher BPA uptake by proliferating cells than by quiescent cells. The boron concentration determined in the same number of cells was higher in the G2/M cells than in the G0/G1 cells concluding that BPA uptake was dependent on the cell cycle. Another in vitro study, on the localization of ^{10}B (BPA) in metaphase and interphase T98G human glioblastoma cells, using secondary ion mass spectrometry (SIMS), reported reduced levels of ^{10}B in the cytoplasm of mitotic cells compared with interphase cells (Chandra et al. 2008). Nevertheless, Detta and Cruickshank (2009) reasoned that if the BPA uptake by tumor cells was coupled to their proliferation status, then BPA-based BNCT would have a very low efficacy because the only cells targetable would be the ones temporally in cycle in the tumor. In the study both authors reported, based on the analysis of the amino acid transporter LAT1, that a large proportion of the tumor cells were available for BNCT regardless of the cell cycle status. Furthermore, the study also reported that BPA-based BNCT might affect an average 70% of detected tumor cells, which is three times the proportion suggested by their cell cycle status.

Considering the diversity of results obtained in the studies on the BPA uptake and its relation to the cell cycle more studies are needed in order to clarify this issue.

There are also reports in the literature where intracellular melanin levels were measured and correlated to effects of BNCT. Melanomas and metastatic melanoma in particular are known to vary considerably in the degree of pigmentation. In the cutaneous melanoma treatments with BNCT the boron carrier must be administered systemically and be capable of delivering boron to both melanotic and amelanotic melanoma in an adequate concentration for effective therapy. The differences in the melanin content between both cell lines chosen for these studies could partly explain the great difference in CBE values obtained for Mel-J and M8 cells. M8 is derived from an amelanotic melanoma, in contrast to Mel-J, which was established from a pigmented metastatic lesion. Previous studies have reported that amelanotic melanomas exhibit relatively lower BPA accumulation than melanin producing melanomas and presented a more active efflux of BPA than pigmented melanomas (Mishima et al. 1989, Fukuda et al. 1994). Coderre and co-workers studied the tumor uptake of BPA in both pigmented and non-pigmented melanomas and found that the tumor uptake of boron in amelanotic melanomas was about 50% of that observed in well pigmented counterparts. Nonetheless, the BPA was still selectively concentrated in the amelanotic tumor cells in comparison to normal cells and in sufficient concentrations for effective BNCT (Coderre et al. 1990). Hence, our results obtained for the effectiveness factors and previous uptake assays (Carpano et al. 2010) might suggest that the differences between the CBE values for both cell lines are related to the activity of BPA transport and/or the degree of loss caused by the efflux of BPA before and during irradiation.

The results of number of tracks determined by neutron-induced α-autoradiography might be reflecting these differences of uptake/efflux of ^{10}B between the amelanotic and the pigmented cell line. Moreover, intracellular boron seems to be accumulated at relative high concentrations in Mel-J cells, more than twice the extracellular concentration if we consider the results of intracellular and extracellular track densities ratios (Figure 4).

Considering the above-mentioned ratios and our assumption of equivalent ^{10}B concentrations between extracellular and intracellular compartments during dosimetry determinations, we should mention that the CBE factors determined might be slightly overestimated, especially for Mel-J cells.

Another noteworthy point is that considering the broad differences in radiosensitivities obtained from the survival curves using conventional gamma radiation; it is remarkable how the in vitro BNCT treatments tend to reduce the gap between survival fraction values as a function of total physical absorbed dose in both cell lines. This reduction suggests greater independence between the response to radiation during BNCT and the intrinsic radioresponsiveness of both cell lines compared to the dose-response in conventional low-LET photon radiotherapy. The dose-response in low-LET modalities is strongly dependent upon intrinsic radioresistance of cells, as shown in Figures 1 and 2. It seems that the higher the LET, the greater the level of independence between the variability in radioresponsiveness of tumor cells. This suggests that the broad variation during dose prescription in conventional photon radiotherapy could be a minor problem in BNCT treatments, providing optimal therapeutic dosage while minimizing collateral effects on healthy tissue.

The dose values obtained as a result of the simulation with the NCTP treatment planning system and the DVH Tool system, implementing the RBE and CBE factors obtained in vitro, would confirm that prescribing the minimum tolerable dose (MTB) for skin amply surpasses the minimum dose required for tumor control. Conveniently, this is even more so for the more radioresistant cell line Mel-J, suggesting an even wider margin of success.

However, it is important to mention that regarding the uncertainty of total absorbed doses from the measurements of thermal neutron fluencies, based on the expression (3) developed by Coderre et al. (1993), we assume that each component of the radiation was simply additive, even though it has been reported that the effects of mixed radiations of high and low LET are at least synergistic. Moreover, it has been reported that these components might interact in a much more complex manner (Santa Cruz and Zamenhof 2004).

Finally, despite the success of the implementation of the in vitro effectiveness factors, it is worth mentioning that in the CBE calculations of the ^{10}B (n,α) ^{7}Li reaction, we assumed that BPA is uniformly distributed inside and outside the cells. However, autoradiographic images showed marked differences for ^{10}B uptake between both cell lines and between cells and the concentration of ^{10}B in culture media as well. The findings recently published by Chandra and collaborators on B16 cells demonstrated that uptake of cis-ABCPC, a synthetic boronated aminoacid, is time-dependent with a 7.5:1 partitioning ratio of boron between cell nuclei and the nutrient medium after 4 h incubation (Chandra et al. 2013).

All these findings revealed the importance of developing more detailed studies on the dependence of CBE on ^{10}B microdistribution within cells, and confirmed the need for a deeper knowledge on the role for all the subunits of system L amino acid transporters responsible of BPA uptake.

Conclusions

The present studies provide the first RBE values with our nuclear reactor and are the first to provide data on CBE values for melanoma using BPA as the boron carrier. These data will hopefully help to optimize future treatments in Argentina. However, it must be emphasized that ^{10}B distribution at the subcellular level requires further study and more accurate values of intracellular ^{10}B concentrations to be determined in order to make the effectiveness factors more realistic in the clinical BNCT field.

Acknowledgements

The authors thank Gustavo Santa Cruz and Sara Gonzalez for constructively criticizing the drafts of this manuscript and for helpful scientific discussions. This study was conducted with grants from CONICET, ANPCYT, and the School of Medicine of the University of Buenos Aires. We also thank Dr Sara Liberman (National Atomic Energy Commission) for her continuous support.

Declaration of interest

The authors report no conflicts of interest. The authors alone are responsible for the content and writing of the paper.

References

Amemiya K, Takahashi H, Kajimoto Y, Nakazawa M, Yanagie H, Hisa T, Eriguchi M, Nakagawa Y, Majima T, Kageji T, Sakurai Y, Kobayashi T, Konishi T, Hieda K, Yasuda N, Ogura K. 2005. High-resolution nuclear track mapping in detailed cellular histology using CR-39 with the contact microscopy technique. Radiat Measure 40:283–288.

Babu E, Kanai Y, Chairoungdua A, Kim DK, Iribe Y, Tangtrongsup S, Jutabha P, Li Y, Ahmed N, Sakamoto S, Anzai N, Nagamori S, Endou H. 2003. Identification of a novel system L amino acid transporter structurally distinct from heterodimeric amino acid transporters. J Biologic Chem 278:43838–43845.

Barth RF, Coderre JA, Vicente MGH, Blue TE. 2005. Boron neutron capture therapy of cancer: Current status and future prospects. Clin Cancer Res 11:3987–4002.

Barth RF, Vicente MG, Harling OK, Kiger WS 3rd, Riley KJ, Binns PJ, Wagner FM, Suzuki M, Aihara T, Kato I, Kawabata S. 2012. Current status of boron neutron capture therapy of high grade gliomas and recurrent head and neck cancer. Radiat Oncol 7: 146–166.

Blaumann HR, González SJ, Longhino J, Santa Cruz GA, Calzetta Larrieu OA, Bonomi MR, Roth BM. 2004. Boron neutron capture therapy of skin melanomas at the RA-6 reactor: A

procedural approach to beam set up and performance evaluation for upcoming clinical trials. Med Phys 31:70–80. Erratum in: Med Phys 2004;31:2373.

Bodoy S, Martín L, Zorzano A, Palacín M, Estévez R, Bertran J. 2005. Identification of LAT4, a novel amino acid transporter with system L activity. J Biologic Chem 280:12002–12011.

Carpano M, Dagrosa A, Nievas S, Rossini A, Juvenal G, Pisarev M. 2010. Comparative studies of boronophenylalanine (BPA) uptake in three human cell lines of malignant melanoma. Proceedings of 14th International Congress on Neutron Capture Therapy, October 25–29, Buenos Aires, Argentina. pp 123–125.

Chandra S, Tjarks W, Lorey DR 2nd, Barth RF. 2008. Quantitative subcellular imaging of boron compounds in individual mitotic and interphase human glioblastoma cells with imaging secondary ion mass spectrometry (SIMS). J Microscopy 229:92–103.

Chandra S, Barth RF, Haider SA, Yang W, Huo T, Shaikh AL, Kabalka GW. 2013. Biodistribution and subcellular localization of an unnatural boron-containing amino acid (cis-ABCPC) by imaging secondary ion mass spectrometry for neutron capture therapy of melanomas and gliomas. PLoS One 8:e75377.

Coderre JA, Glass JD, Packer S, Micca P, Greenberg D. 1990. Experimental boron neutron capture therapy for melanoma: Systemic delivery of boron to melanotic and amelanotic melanoma. Pigment Cell Res 3:310–318.

Coderre JA, Morris GM. 1999. The radiation biology of boron neutron capture therapy. Radiat Res 151:1–18.

Coderre JA, Turcotte JC, Riley KJ, Binns PJ, Harling OK, Kiger WS 3rd. 2003. Boron neutron capture therapy: Cellular targeting of high linear energy transfer radiation. Technol Cancer Res Treat 2: 355–375.

Dean E, Lorigan P. 2012. Advances in the management of melanoma: targeted therapy, immunotherapy and future directions. Expert Rev Anticancer Ther 12:1437–1448.

Detta A, Cruickshank GS. 2009. L-amino acid transporter-1 and boronophenylalanine-based boron neutron capture therapy of human brain tumors. Cancer Res 69:2126–2132.

Franken APN, Rodermond HM, Stap J, Haveman J, van Bree C. 2006. Clonogenic assay of cells *in vitro*. Nature Protocols 1: 2315–2319.

Fukuda H, Hiratsuka J, Honda C, Kobayashi T, Yoshino K, Karashima H, Takahashi J, Abe Y, Kanda K, Ichihashi M, Mishima Y. 1994. Boron neutron capture therapy of malignant melanoma using B-10-paraboronophenylalanine with special reference to evaluation of radiation dose and damage to the normal skin. Radiat Res 138:435–442.

Fukuda H, Hiratsuka J, Kobayashi T, Sakurai Y, Yoshino K, Karashima H, Turu K, Araki K, Mishima Y, Ichihashi M. 2003. Boron Neutron Capture Therapy (BNCT) for malignant melanoma with special reference to absorbed doses to the normal skin and tumor. Australas Phys Engineer Sci Med 26:97–103.

González SJ, Bonomi MR, Santa Cruz GA, Blaumann HR, Calzetta Larrieu OA, Menéndez P, Jiménez Rebagliati R, Longhino J, Feld DB, Dagrosa MA, Argerich C, Castiglia SG, Batistoni DA, Liberman SJ, Roth BM. 2004. First BNCT treatment of a skin melanoma in Argentina: Dosimetric analysis and clinical outcome. Appl Radiat Isotopes 61:1101–1105.

Gray-Schopfer V, Wellbrock C, Marais R. 2007. Melanoma biology and new targeted therapy. Nature 445:851–857.

Guerra L, Mordoh J, Slavutsky I, Larripa I, Medrano EE. 1989. Characterization of IIB-MEL-J: A new and highly heterogenous human melanoma cell line. Pigment Cell Melanoma Res 2: 504–509.

Imahori Y, Ueda S, Ohmori Y, Sakae K, Kusuki T, Kobayashi T, Takagaki M, Ono K, Ido T, Fujii R. 1998. Positron emission tomography-based boron neutron capture therapy using boronophenylalanine for high-grade gliomas: Parts I and II. Clin Cancer Res 4:1825–1832 (part I); 1833–1841(II).

Kaira K, Sunose Y, Ohshima Y, Ishioka NS, Arakawa K, Ogawa T, Sunaga N, Shimizu K, Tominaga H, Oriuchi N, Itoh H, Nagamori S, Kanai Y, Yamaguchi A, Segawa A, Ide M, Kaira K, Oriuchi N, Imai H, Shimizu K, Yanagitani N, Sunaga N, Hisada T, Ishizuka T, Kanai Y, Endou H, Nakajima T, Mori M. 2009. Prognostic significance of L-type amino acid transporter 1 (LAT1) and 4F2 heavy chain (CD98) expression in early stage squamous cell carcinoma of the lung. Cancer Sci 100:248–254.

Kanai Y, Segawa H, Miyamoto K, Uchino H, Takeda E, Endou H. 1998. Expression cloning and characterization of a transporter for large neutral amino acids activated by the heavy chain of 4F2 antigen (CD98). J Biologic Chem 273:23629–23632

Konishi T, Amemiya K, Natsume T, Takeyasu A, Yasuda N, Furusawa Y, Hieda K. 2007. A new method for the simultaneous detection of mammalian cells and ion tracks on a surface of CR-39. J Radiat Res 48:255–261.

Loria D, González A, Latorre C. 2008. Cutaneous melanoma epidemiology in Argentina: Analysis from the Argentine Cutaneous Melanoma Registry. Dermatol Argentina 14:436–443.

Mackiewicz-Wysocka M, Zolnierek J, Wysocki PJ. 2013. New therapeutic options in systemic treatment of advanced cutaneous melanoma. Expert Opin Investigat Drugs 22:181–190.

Menéndez PR, Roth BMC, González SJ, Santa Cruz GA, Blaumann HR, Calzetta Larrieu OA, Feld D, Casal MR, Jimenez Rebagliati R, Nievas SI, Longhino J, Pereira MD, Fernandez CD, Kessler J, Liberman SJ. 2009. BNCT for skin melanoma in extremities: updated argentine clinical results. Appl Radiat Isotopes 67:50–53.

Miller M, Quintana J, Ojeda J, Langan S, Thorp S, Pozzi E, Sztejnberg M, Estryk G, Nosal R, Saire E, Agrazar H, Graiño F. 2009. New irradiation facility for biomedical applications at the RA-3 reactor thermal column. Appl Radiat Isotopes 67:226–229.

Mishima Y, Ichihashi M, Hatta S, Honda C, Yamamura K, Nakagawa T. 1989. New thermal neutron capture therapy for malignant melanoma: Melanogenesis-seeking 10B molecule-melanoma cell interaction from in vitro to first clinical trial. Pigment Cell Melanoma Res 2:226–234.

Ono K, Masunaga SI, Kinashi Y, Takagaki M, Akaboshi M, Kobayashi T, Akuta K. 1996. Radiobiological evidence suggesting heterogeneous microdistribution of boron compounds in tumors: Its relation to quiescent cell population and tumor cure in neutron capture therapy. Int J Radiat Oncol Biol Phys 34:1081–1086.

Papaspyrou M, Feinendegen LE, Müller-Gärtner HW. 1994. Preloading with L-tyrosine increases the uptake of boronophenylalanine in mouse melanoma cells. Cancer Res 54:6311–6314.

Pineda M, Fernández E, Torrents D, Estévez R, López C, Camps M, Lloberas J, Zorzano A, Palacín M. 1999. Identification of a membrane protein, LAT-2, that co-expresses with 4F2 heavy chain, an L-type amino acid transport activity with broad specificity for small and large zwitterionic amino acids. J Biologic Chem 274: 19738–19744.

Rigel DS. 2010. Epidemiology of melanoma. Semin Cutan Med Surgery 29:204–209.

Rofstad EK. 1992. Radiation sensitivity *in vitro* of primary tumours and metastatic lesions of malignant melanoma. Cancer Res 52: 4453–4457.

Rossini AE, Thomasz L, Dagrosa MA, Carpano M, Juvenal G, Pisarev M. 2010. Molecular characterization of amino acid transporter system L involved in boronophenylalanine uptake for BNCT in melanoma. Proceedings of 14th International Congress on Neutron Capture Therapy, October 25–29, Buenos Aires, Argentina. pp 123–125.

Santa Cruz GA, Zamenhof RG. 2004. The microdosimetry of the (10) B reaction in boron neutron capture therapy: A new generalized theory. Radiat Res 162:702–710.

Selzer E, Hebar A. 2012. Basic principles of molecular effects of irradiation. Wiener Medizin Wochenschrift 162:47–54.

Suzuki M, Masunaga SI, Kinashi Y, Takagaki M, Sakurai Y, Kobayashi T, Ono K. 2000. The effects of boron neutron capture therapy on liver tumors and normal hepatocytes in mice. Japan J Cancer Res 91:1058–1064.

van den Aardweg GJ, Naus NC, Verhoeven AC, de Klein A, Luyten GP. 2002. Cellular radiosensitivity of primary and metastatic human uveal melanoma cell lines. Investig Ophthalmol Visual Sci 43:2561–2565.

Wambersie A, Menzel HG. 1993. RBE in fast neutron therapy and in boron neutron capture therapy. A useful concept or a misuse? Strahlentherapie und Onkologie 169:57–64.

Wittig A, Sauerwein WA, Coderre JA. 2000. Mechanisms of transport of p-borono-phenylalanine through the cell membrane *in vitro*. Radiat Res 153:173–180.

Yanagisawa N, Ichinoe M, Mikami T, Nakada N, Hana K, Koizumi W, Endou H, Okayasu I. 2012. High expression of L-type amino acid transporter 1 (LAT1) predicts poor prognosis in pancreatic ductal adenocarcinomas. J Clin Pathol 65:1019–1023.

Yoshida F, Matsumura A, Shibata Y, Yamamoto T, Nakauchi H, Okumura M, Nose T. 2002. Cell cycle dependence of boron uptake from two boron compounds used for clinical neutron capture therapy. Cancer Lett 187:135–141.